




# Potential biomarkers and lncRNA-mRNA regulatory networks in invasive growth hormone-secreting pituitary adenomas

H. Yin<sup>1</sup> · X. Zheng<sup>1</sup> · X. Tang<sup>1</sup> · Z. Zang<sup>1</sup> · B. Li<sup>3</sup> · S. He<sup>1</sup> · R. Shen<sup>2</sup> · H. Yang<sup>1</sup> · S. Li<sup>1</sup> 

Received: 14 April 2020 / Accepted: 15 January 2021  
© Italian Society of Endocrinology (SIE) 2021

## Abstract

**Purpose** Growth hormone-secreting pituitary adenomas (GH-PAs) are common subtypes of functional PAs. Invasive GH-PAs play a key role in restricting poor outcomes. The transcriptional changes in GH-PAs were evaluated.

**Methods** In this study, the transcriptome analysis of six different GH-PA samples was performed. The functional roles, co-regulatory network, and chromosome location of differentially expressed (DE) genes in invasive GH-PAs were explored.

**Results** Bioinformatic analysis revealed 101 DE mRNAs and 70 DE long non-coding RNAs (lncRNAs) between invasive and non-invasive GH-PAs. Functional enrichment analysis showed that epithelial cell differentiation and development pathways were suppressed in invasive GH-PAs, whereas the pathways of olfactory transduction, retinol metabolism, drug metabolism-cytochrome P450, and metabolism of xenobiotics by cytochrome P450 had an active trend. In the protein–protein interaction network, 11 main communities were characterized by cell- adhesion, -motility, and -cycle; transport process; phosphorus and hormone metabolic processes. The *SGK1* gene was suggested to play a role in the invasiveness of GH-PAs. Furthermore, the up-regulated genes *OR51B6*, *OR52E4*, *OR52E8*, *OR52E6*, *OR52N2*, *MAGEA6*, *MAGEC1*, *ST8SIA6-AS1*, and the down-regulated genes *GAD1-AS1* and *SPINT1-AS1* were identified in the competing endogenous RNA network. The RT-qPCR results further supported the aberrant expression of those genes. Finally, the enrichment of DE genes in chromosome 11p15 and 12p13 regions were detected.

**Conclusion** Our findings provide a new perspective for studies evaluating the underlying mechanism of invasive GH-PAs.

**Keywords** Growth hormone-secreting pituitary adenoma · mRNAs · Long non-coding RNAs · Differentially expressed genes · Bioinformatics

## Introduction

Pituitary adenoma (PA) is a common intracranial primary tumor accounting for 10–15% of all intracranial tumors [1]. Growth hormone-secreting pituitary adenomas (GH-PAs) are common subtypes of functional adenomas. Excessive secretion of growth hormone may lead to acromegaly, heart disease, sleep apnea, and other diseases that can reduce the life expectancy of patients by approximately 10 years. Although most GH-PAs are morphologically characterized as benign tumors, 49.7% of GH-PAs invade the surrounding cavernous sinus, sphenoid sinus, and neighboring structures. Thus, invasive GH-PAs show biological characteristics similar to those of malignant tumors [2]. Patients with invasive GH-PAs often present a low rate of total surgical resection, a high rate of tumor recurrence, and poor prognosis [3]. Therefore, studying the invasion mechanism of GH-PAs is

Huachun Yin and Xin Zheng, Xiaoshuang Tang have contributed equally to this work.

**Supplementary Information** The online version contains supplementary material available at <https://doi.org/10.1007/s40618-021-01510-x>.

✉ H. Yang  
huiyangtg2018@aliyun.com

✉ S. Li  
dlisong3@163.com

- <sup>1</sup> Department of Neurosurgery, Xinqiao Hospital, The Army Medical University, Chongqing, China
- <sup>2</sup> Department of Endocrinology, Xinqiao Hospital, The Army Medical University, Chongqing, China
- <sup>3</sup> College of Life Sciences, Chongqing Normal University, Chongqing, China

important for evaluating and making an accurate prognosis for patients with GH-PAs.

To explore the invasion mechanism of GH-PAs, chromosomal alterations, oncogenes, tumor suppressor genes, proliferation markers, growth factors and their receptors, angiogenic markers, and cell adhesion molecules have been investigated [4]. However, not a single molecule has been identified and widely accepted to predict or explain the invasiveness of GH-PAs. In our previous studies, we found that viral infection [5] and dysregulation of lactate dehydrogenase A [6] increased the invasiveness of GH-PAs tumor cells, whereas other studies showed different results [4]. Therefore, a more comprehensive tool such as the use of bioinformatic technologies is needed to examine the genes and RNA changes in invasive GH-PAs.

RNA-sequencing (RNA-seq) can be used for high-resolution transcriptomics analysis [7]. According to the open-source database search of NCBI GEO [8] and GTEx [9], only two RNA-seq datasets for GH-PAs were identified [10, 11], and no detailed study on the invasive GH-PAs was performed. Thus, the studies investigating the mRNA and long non-coding RNA (lncRNA) levels in invasive GH-PAs are lacking.

RNA-seq analysis was performed to identify changes in gene expression, gene-related regulation networks during GH-PAs invasion, and potential molecules involved in the invasiveness of GH-PAs. Differentially expressed (DE) mRNAs and lncRNAs were detected between invasive and non-invasive GH-PAs. Functional annotations, protein–protein interactions (PPI), and competing endogenous (ceRNA) networks were created. The chromosome location enrichment was conducted to examine the underlying molecular mechanisms of invasive GH-PAs. The potential biomarkers were verified by real-time fluorescent quantitative PCR (RT-qPCR).

## Materials and methods

### Sample collection

Samples used in this study were collected from six patients with GH-PAs who underwent transsphenoidal surgery at the Xinqiao Hospital in Chongqing, China. GH-PAs were diagnosed according to clinical and hormonal evaluation and additional information provided by pathological assessment confirmed the diagnoses. Tumor invasiveness was determined based on magnetic resonance imaging scans using the modified Knosp criteria combined with intraoperative findings. Among the six patients, three had invasive and three had non-invasive adenomas (summarized in Table 1). This study was approved by the Ethics and Clinical Research Committee of Xinqiao Hospital and a written informed consent was obtained from each patient.

### Library preparation and sequencing

All tumor samples obtained during surgery were immediately placed in TRIzol (Invitrogen, Carlsbad, CA, USA) and maintained at  $-20^{\circ}\text{C}$  until RNA extraction. Total RNA was isolated from the tissues according to the manufacturer's instructions. The quantity and quality of the total RNA were evaluated using a ND-1000 Nanodrop spectrophotometer (NanoDrop Technologies, Wilmington, DE, USA). Each RNA sample had an A260/A280 ratio above 1.80 and an A260/A230 ratio above 2.00. RNA integrity was evaluated using the Agilent 2200 TapeStation (Agilent Technologies, Santa Clara, CA, USA) and each sample had an RINe above 7.0. Next, rRNA was removed from total RNA by using the Epicenter Ribo-Zero rRNA Removal Kit (Illumina, San Diego, CA, USA) and was fragmented into approximately 200 bp fragments. The purified RNAs were subjected to first-strand and second-strand cDNA synthesis followed by adaptor ligation and enrichment with a low-cycle, according to the TruSeq<sup>®</sup> RNA LT/HT Sample Prep Kit (Illumina) instructions. The purified library products were evaluated using the Agilent 2200 TapeStation and Qubit<sup>®</sup> 2.0 (Life Technologies, Carlsbad, CA, USA) and then diluted to

**Table 1** Patient information

Patient ID	Age	Sex	Knosp Grade	Tumor Size (cm)	Ki-67	GH (random/ nadir in OGTT)	IGF-1
1	36	Female	K4	2.2 × 2.5 × 2.4	1%	> 40/37.2	1231
2	43	Female	K3	1.9 × 2.6 × 2.9	7%	39.8/20.4	900
3	16	Male	K3	2.8 × 3.4 × 2.8	5%	> 40/32.5	784
4	59	Male	K1	1.5 × 1.7 × 1.6	4–6%	> 40/18.6	688
5	52	Female	K2	1.5 × 1.9 × 2.2	4%	7.66/4.32	708
6	46	Female	K2	1.4 × 1.7 × 1.0	(–)	> 40/26.3	495

10 pM for in situ cluster generation on the HiSeq 2500 pair-end flow cell. Sequencing ( $2 \times 100$  bp) was performed on the HiSeq 2500.

### Mapping of sequencing reads

Six libraries from invasive and non-invasive acromegalic tissues were analyzed on the Illumina HiSeq platform. DynamicTrim Perl script, implemented with the help of SolexaQA package [12], was used to control the quality of the raw sequencing data according to the following criteria: (1) sequencing reads containing adaptors were removed; (2) artificial reads were removed; (3) nucleotides with a quality-score lower than 20 were removed. The cleaned sequencing reads were then aligned to the GRCh38 genome using TopHat (v1.0.12) BWA software [13].

### Identification of DE mRNA and lncRNA

The transcription abundance of each gene was accessed by Cufflinks (v1.0.3) [14]. The gene transfer format file for the reference genome annotation used in this analysis was retrieved from the UCSC database [15]. Protein-coding and long non-coding genes annotated in GENCODEv27 were retained. After filtering non-expressed or low-expressed genes, genes with counts per million value greater than one remained in at least six libraries. The data was normalized into fragments per kilobase of exon model per million mapped fragments values. To confirm that our samples are not contaminated with normal pituitary or other PAs, we reanalyzed the transcriptome data and found the tumor samples in our study presented high expression levels of Pit1, but very low expression levels of SF-1 and T-PIT (Figure S1 A), which supported our tumor samples were somatotroph adenomas according to 2017 WHO classification of PAs [16]. Then, DE genes were identified between invasive and non-invasive GH-PAs using the edgeR R package [17]. Genes with a fold-change (FC)  $> 2$  and false discovery rate (FDR)  $< 0.05$  were considered DE genes between invasive and non-invasive GH-PAs.

### Functional annotations and enrichment analysis of DE mRNAs

For functional annotation of the DE mRNAs, the gene ontology (GO) and Kyoto Encyclopedia of Genes and Genomes (KEGG) pathways enrichment analyses were conducted using the ToppGene web server and the results were considered significant for  $p$  values  $< 0.05$  [18]. To identify overexpressed and under-expressed genes based on the DE mRNAs, the Z-score was calculated in each term using the following formula [19, 20]:

$$Z\text{-score} = \frac{N_{\text{up}} - N_{\text{down}}}{\sqrt{\text{count}}}$$

The  $N_{\text{up}}$  and  $N_{\text{down}}$  represent the number of up-regulated and down-regulated genes between invasive and non-invasive tumor, respectively, while the count indicates the number of DE mRNAs in each term.

### Construction of protein–protein interaction network and community detection

To explore the potential protein–protein interaction associated with invasive GH-PAs, the list of DE mRNAs was mapped on the IMEx Interactome and STRING online database (confidence score cutoff  $> 700$ ), which has a built-in NetworkAnalyst [21]. Communities in the PPI network were detected using the InfoMap algorithm and were visualized using Cytoscape (v3.6) [22].

### Construction of the ceRNA network

The mRNA–miRNA pairs were predicted using the ToppGene Suite (TargetScan, miRTarbase, and MSigDB databases), with a threshold of Benjamini and Hochberg adjustment (adj.)  $p$  value  $< 0.01$ . The lncRNA–miRNA pairs were chosen based on a threshold of  $p$  value  $< 0.01$ .

The correlation between DE mRNAs and DE lncRNAs was evaluated using Pearson's correlation coefficient (PCC) algorithm on the matched mRNAs and lncRNAs expression profile data:

$$PCC = \frac{1}{n-1} \sum_{i=1}^n \left( \frac{\text{mRNA}_i - \overline{\text{mRNA}}}{\partial(\text{mRNA})} \times \frac{\text{lncRNA}_i - \overline{\text{lncRNA}}}{\partial(\text{lncRNA})} \right)$$

Where  $n$  is the number of samples,  $\text{mRNA}_i$  is the expression value of mRNA in sample  $i$ ,  $\overline{\text{mRNA}}$  is the average expression level of mRNA in all samples, and  $\partial(\text{mRNA})$  represents the standard deviation of mRNA expression level. These notations apply to the lncRNA as well. To reduce the possibility of false-positives, only the mRNA–lncRNA pairs with a  $PCC > |0.70|$  and adj.  $p$  value  $< 0.01$  were further analyzed [23]. The miRNA–lncRNA–mRNA interaction pairs were visualized in Cytoscape software.

To further explore the miRNA–lncRNA–mRNA interaction pairs associated with invasive GH-PAs, the *cytoHubba*, a Cytoscape plugin, was used to calculate high-degree genes [24], and the *MCODE*, another Cytoscape plugin, was used to screen for notable modules in the ceRNA network [25]. The following advanced options parameters were set for the *MCODE* plugin: degree cutoff = 3; node score cutoff = 0.2; K-score = 5. Modules with scores  $> 3$  and nodes  $> 6$  were identified as significant modules.

## Chromosomal position effect on gene expression

To determine whether the chromosomal position affected gene expression patterns in invasive GH-PAs, all DE mRNAs and DE lncRNAs were mapped and enriched on chromosomes using the GSEA online tool [26]. The results were visualized using the KaryoploteR package [27].

## RNA-Seq data validation by RT-qPCR

To exclude the interference from normal pituitary tissue and another type of PAs, the known GH-PAs transcription factor (T-PIT, Pit1, SF-1) was confirmed by RT-qPCR. The results show that only the Pit1 has a relatively high expression compared with normal pituitary (Figure S1 B). Meanwhile, the expression of eleven genes (*SGK1*, *OR51B6*, *OR52E4*, *OR52E8*, *OR52E6*, *OR52N2*, *MAGEA6*, *MAGEC1*, *ST8SIA6-AS1*, *SPINT1-AS1*, and *GAD1-AS*) obtained from the RNA-seq data were confirmed by RT-qPCR.

Primers were designed using Beacon Designer 7.0 software (Premier Biosoft International, Palo Alto, CA, USA), and the sequences are listed in Supplementary Table S1. Total RNA samples were reverse transcribed into cDNAs using the SuperScript First-Strand Synthesis System (Invitrogen, Carlsbad, CA, USA). A CFX96 Real-time System (Bio-Rad Laboratories) and TB Green Premix Ex Taq II (TaKaRa, RR820A) were used to perform RT-qPCR. The relative gene expression levels were calculated using the  $2^{-\Delta\Delta CT}$  method with GAPDH gene as the internal control [28]. To ensure comparability of the RT-qPCR assays, the calculation of amplifying efficiency of each primer

according to  $[E = [10^{-(1/\text{slope})} - 1] \times 100\%$  with five dilution points. Each experiment was carried out in triplicate. All analysis process is shown in Fig. 1.

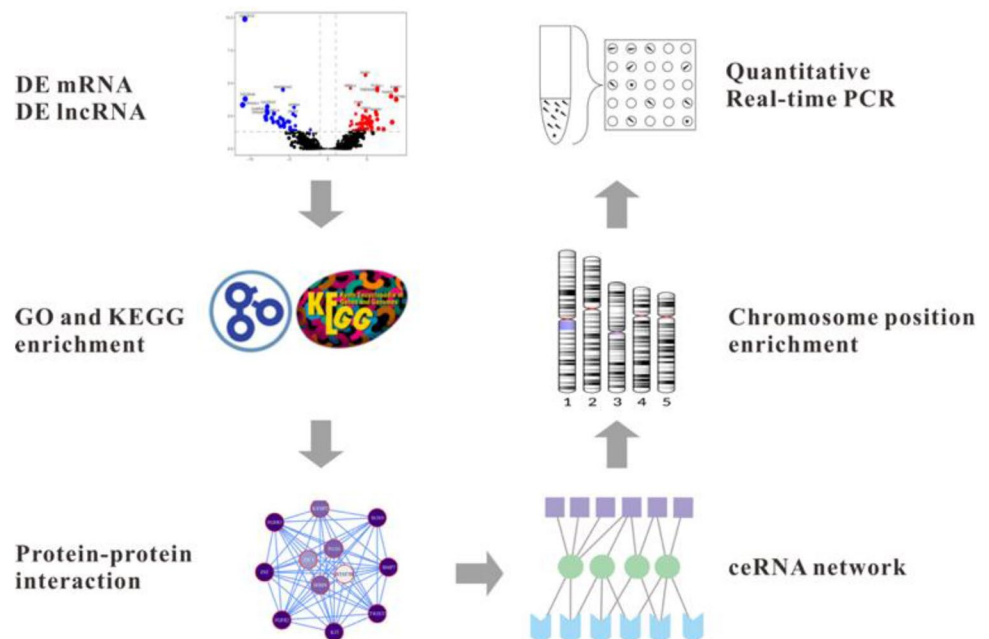
## Results

### Transcriptome sequencing by RNA-seq and identification of DE genes

To comprehensively analyze the transcriptome of invasive tumor tissues, DE genes associated with the invasion of GH-PAs were identified. We used an Illumina HiSeq 2500 platform with a pair-end flow cell followed by sequencing ( $2 \times 100$  bp) of the whole transcriptome. Finally, following quality control, an average of 152.34 million reads per sample were obtained which sufficiently covered the transcriptome profile. The rate of sequencing readings mapped to the human reference genome met the quality standards of the RNA-seq technique. Hence, our RNA-seq dataset provided a good representation of the expressed genes in the human genome.

The volcano plot of DE mRNA (Fig. 2) and DE lncRNAs (Fig. 3) were represent data obtained from the invasive and non-invasive tumor mRNA and lncRNA sequencing, respectively. Among them, 64 up-regulated and 37 down-regulated mRNAs with a  $|\log FC| > 2$  and  $FDR < 0.05$  were identified. Furthermore, 46 up-regulated and 24 down-regulated lncRNAs transcripts from 42 genes were identified.

**Fig. 1** Workflow of DE genes analyzed in this study





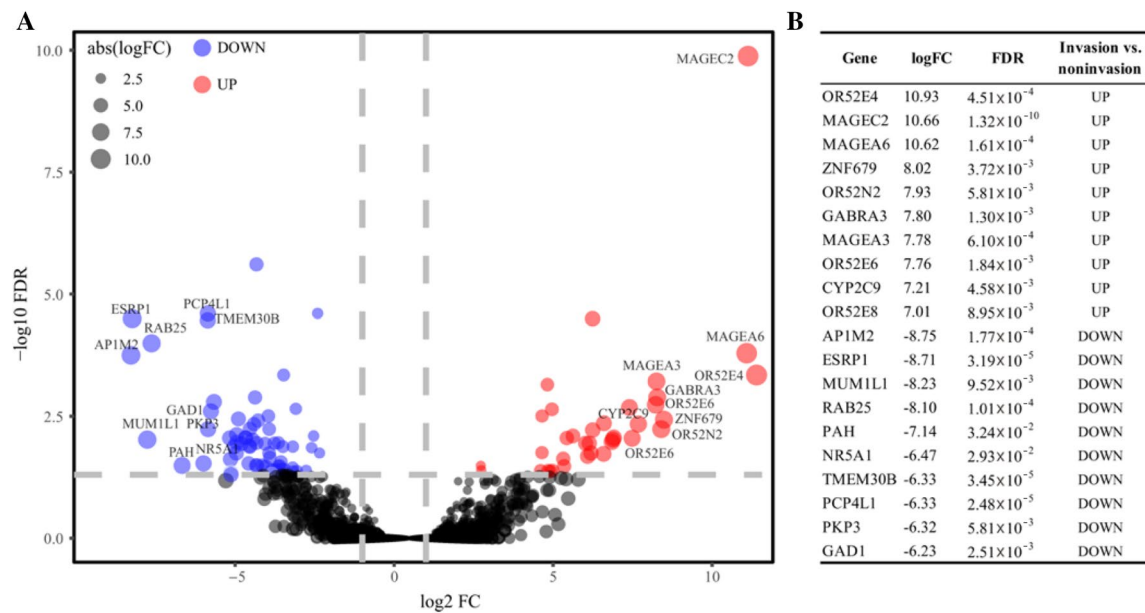


**Fig. 2** DE mRNAs in invasive GH-PAs. **a** Volcano plot of DE mRNAs. Blue circles indicate down-regulated genes and red circles indicate up-regulated genes. **b** Top ten up-regulated and down-

regulated DE mRNAs. The dashed lines indicate the criterion of DE mRNAs detected. <sup>1</sup>FDR refers to adj. *p*-value returned by the eBayes function in edgeR package

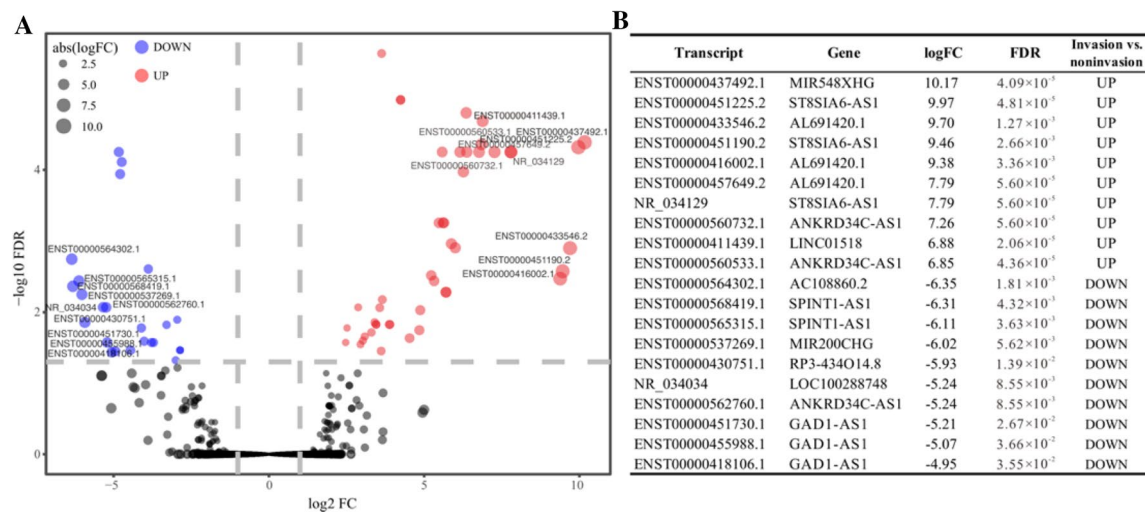


**Fig. 3** DE lncRNAs in invasive GH-PAs. **a** Volcano plot of DE lncRNAs. Blue circles indicate down-regulated genes and red circles indicate up-regulated genes. **b** Top ten up-regulated and down-regulated

DE lncRNAs. The dashed lines indicate the criterion of DE lncRNAs detected. <sup>1</sup>FDR refers to adj. *p* value returned by the eBayes function in edgeR package

## Functional annotations and enrichment analysis

### GO Analysis of DE mRNA

Based on the ToppGene web service analysis (Fig. 4), seven functional terms were significantly enriched with an adj. *p* value < 0.05 (Table 2). Among them, only epithelial cell differentiation (GO:0030855, Z-score = - 2.13) and epithelial

cell development (GO:0002064, Z-score = - 1.88) were enriched in the suppressed biological process. Notably, some metabolism processes in the invasive GH-PAs showed an active trend, including the retinol metabolic process (GO:0042572, Z-score = 2), hormone metabolic process (GO:0042445, Z-score = 0.37), and terpenoid metabolic process (GO:0006721, Z-score = 1.34). Furthermore, the functions of the oxidoreductase activity acceptor (GO:0033695,

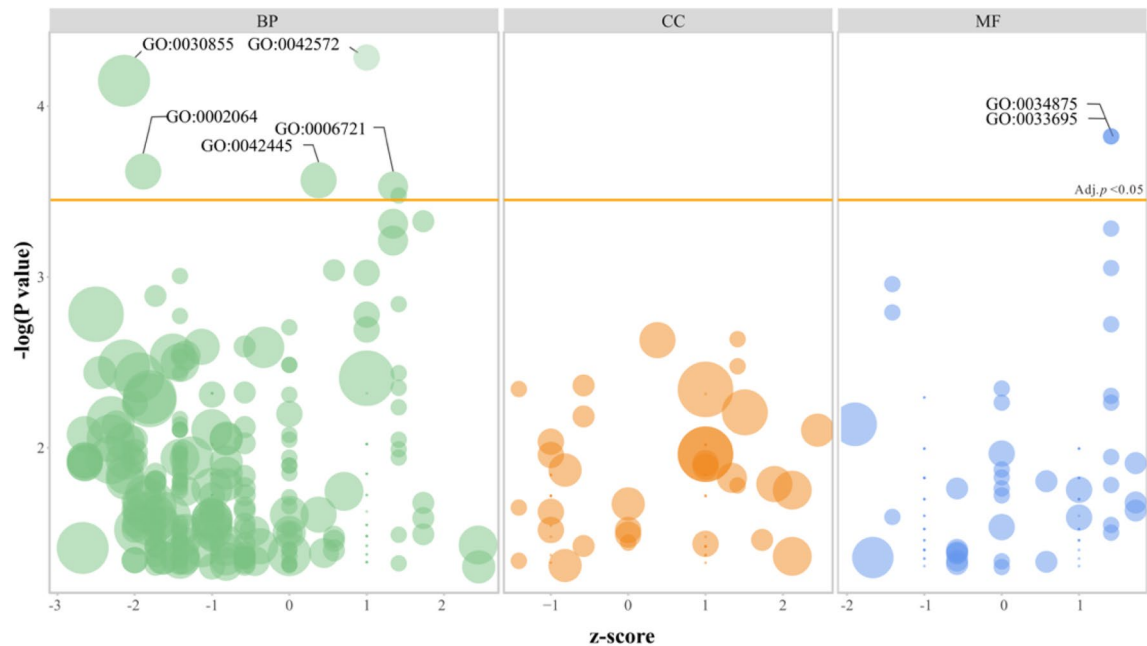


**Fig. 4** GO of DE mRNAs and bubble plot for GO-term enrichment. Bubble size represents the number of DE mRNAs in each GO term. The three levels of GO terms are the biological process (BP), cellular

component (CC), and molecular function (MF). The yellow line indicates the adj.  $p$  value = 0.05

**Table 2** The GO enrichment of the DE mRNA between the invasive and non-invasive GH-PAs

Category	GO Term	Count <sup>1</sup>	Adj. $p^2$	Z-score
BP	GO:0042572 retinol metabolic process	4	$3.74 \times 10^{-2}$	1.00
BP	GO:0030855 epithelial cell differentiation	14	$3.74 \times 10^{-2}$	- 2.13
BP	GO:0002064 epithelial cell development	7	$4.21 \times 10^{-2}$	- 1.88
BP	GO:0042445 hormone metabolic process	7	$4.21 \times 10^{-2}$	0.37
BP	GO:0006721 terpenoid metabolic process	5	$4.43 \times 10^{-2}$	1.34
MF	GO:0034875 caffeine oxidase activity	2	$3.35 \times 10^{-2}$	1.41
MF	GO:0033695 oxidoreductase activity, acting on CH or CH2 groups, quinone or similar compound as acceptor	2	$3.35 \times 10^{-2}$	1.41

<sup>1</sup>Count denotes the number of DE mRNAs in this GO term;

<sup>2</sup>Adj.  $p$  refers to the adjusted  $P$ -value computed by TopGene

Z-score = 1.41) and caffeine oxidase activity (GO:0034875, Z-score = 1.41) were enriched and increased.

### KEGG pathway analysis of DE mRNAs

Based on KEGG pathway mapping (Table 3), the DE mRNAs were significantly enriched in eight pathways with a  $p$  value < 0.05 and gene count  $\geq 4$ . Three of these pathways were involved in metabolism, including retinol metabolism (Z-score = 2), drug metabolism-cytochrome P450 (Z-score = 2), and metabolism of xenobiotics by cytochrome P450 (Z-score = 2). Cytochrome P450 family genes (*CYP2C9* and *CYP3A4*) and alcohol dehydrogenase family genes (*ADH1A* and *ADH1B*) were found

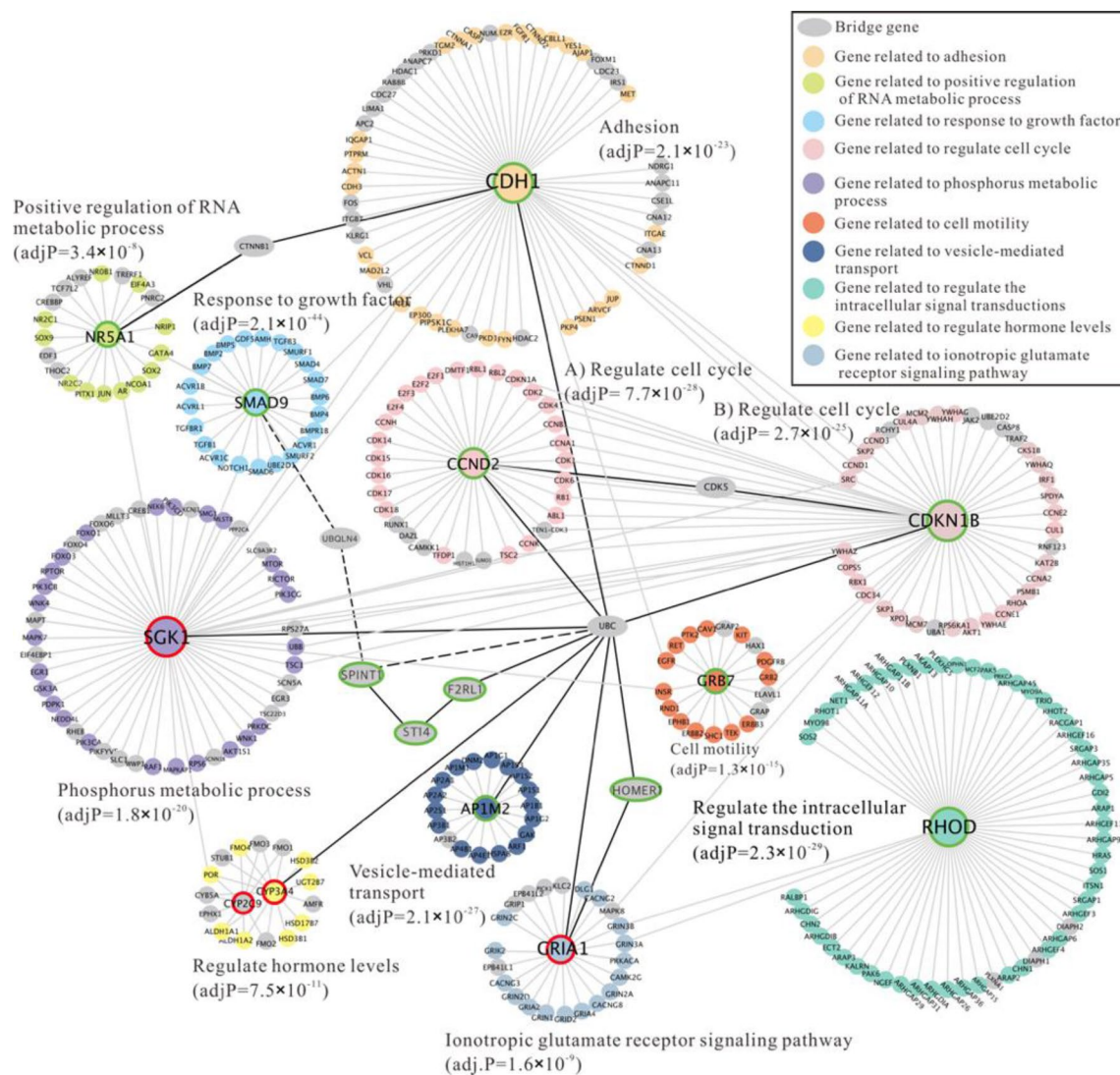
in metabolic disorder-associated pathways. In addition to these metabolism pathways, the neuroactive ligand-receptor interaction pathway (Z-score = 0.37) was also related to invasiveness. Moreover, the olfactory transduction pathway (Z-score = 1.63) was significantly activated, whereas the FOXO signaling pathway (Z-score = - 1) and transcriptional mis-regulation in cancer (Z-score = - 1) were dramatically downregulated in invasive GH-PAs.

### Identification of hub genes based on PPI network construction

To elucidate the mechanisms of molecular regulation in invasive GH-PAs, DE mRNAs were used to construct

**Table 3** The KEGG pathway enrichment of DE mRNAs between the invasive and non-invasive GH-PAs

Description	P-value	Z-score	Gene
hsa83053: Neuroactive ligand-receptor interaction	$7.77 \times 10^{-4}$	0.37	<i>CGA, GRIA1, NMUR2, GIPR, F2RL1, GABBR2, GABRA3</i>
hsa83087: Olfactory transduction	$2.66 \times 10^{-2}$	1.63	<i>SLC8A2, OR51B6, OR52N2, OR52E8, OR52E6, OR52E4</i>
hsa83020: Retinol metabolism	$4.29 \times 10^{-4}$	2.00	<i>CYP2C9, CYP3A4, ADH1A, ADH1B</i>
hsa83032: Drug metabolism-cytochrome P450	$5.69 \times 10^{-4}$	2.00	<i>CYP2C9, CYP3A4, ADH1A, ADH1B</i>
hsa83031: Metabolism of xenobiotics by cytochrome P450	$7.03 \times 10^{-4}$	2.00	<i>CYP2C9, CYP3A4, ADH1A, ADH1B</i>
hsa673221: Chemical carcinogenesis	$1.03 \times 10^{-3}$	2.00	<i>CYP2C9, CYP3A4, ADH1A, ADH1B</i>
hsa921162: FoxO signaling pathway	$5.82 \times 10^{-3}$	-1.00	<i>CDKN1B, SGK1, CCND2, HOMER1</i>
hsa523016: Transcriptional mis-regulation in cancer	$1.68 \times 10^{-2}$	-1.00	<i>CDKN1B, SPINT1, SSX1, CCND2</i>



the PPI network, as visualized by Cytoscape (Fig. 5) via the IMEx interactome and STRING database. To categorize gene functions in different communities, genes with a degree  $\geq 17$  were regarded as hub genes. The network was divided into three groups: hub genes (genes with high interaction with neighboring genes), bridge genes (connecting different communities of neighboring genes), and node genes (connecting with one neighbor).

According to the degree of each node, there were two up-regulated hub genes, *SGK1* (degree = 45) and *GRIA1* (degree = 24), and eight down-regulated hub genes, *RHOD* (degree = 56), *CDKN1B* (degree = 55), *CDH1* (degree = 52), *CCND2* (degree = 33), *SMAD9* (degree = 24), *NR5A1* (degree = 20), and *AP1M2* (degree = 19). For bridge genes, the four down-regulated genes (*SPINT1*, *ST14*, *F2RL1*, and *HOMER1*) were connected to communities.

To explore the functional relationships between DE mRNAs, the network community recognition algorithm InfoMap was used via NetworkAnalyst. Consequently, 11 communities were detected with community nodes  $\geq 19$  and an adj.  $p$  value  $< 0.01$ . Interestingly, the communities, including cell adhesion, cell cycle, intracellular signal transduction, response to growth factor process, cell motility, vesicle-mediated transport process, and RNA metabolic processes were regulated by under-expressed hub genes. The community including phosphorus metabolic process, hormone level regulation process, and ionotropic glutamate receptor signaling pathway contained up-regulated hub genes. These results suggest that the development of invasive GH-PAs might be involved in the disturbance of cellular differentiation and proliferation as well as in the dysregulation of phosphorus metabolic and vesicle-mediated transport.

### LncRNA-miRNA-mRNA network analysis

To predict the relationship between miRNA, DE mRNAs, and DE lncRNAs the ToppGene website was used. A total of 243 nodes (102 miRNAs, 54 lncRNAs, and 86 mRNAs) and 874 edges were analyzed together to construct the ceRNA network. The edges included 264 miRNA-mRNA pairs, 144 miRNA-lncRNA pairs, and 466 lncRNA-mRNA pairs.

The complex ceRNA network showed that DE mRNAs and DE lncRNAs had a highly intricate interaction relationship and together they regulate invasive tumors (Fig. 6a). Based on network features, high-degree genes have a higher importance role than other genes in the network. To detect high-degree genes, all nodes in the ceRNA network were calculated using the *cytoHubba* plugin (nodes with a degree  $> 15$  are listed in Table 4). The results showed that the lncRNA transcripts were mostly accounted for by the 18 nodes with a degree  $> 15$ . Down-regulated *GAD1-AS1* (ENST00000455988.1 and ENST00000418106.1)

showed the strongest correlation with other nodes (degree = 38 and 23 respectively) in the network. The up-regulated *ST8SIA6-AS1* transcripts (ENST00000451225.2, ENST00000451190.2, and ENST00000377597.2) were highly correlated with other genes (degree = 25, 23, and 19 respectively).

CeRNA network module analysis showed that DE mRNAs and DE lncRNAs were highly correlated in the GH-PAs. Based on network module analysis (Fig. 6b), the network clustered into three modules: cluster 1, which had eight genes and 13 edges; cluster 2, which had ten genes and 16 edges with an up-regulated pattern; cluster 3, which had 19 genes and 29 edges with a down-regulated pattern. Genes in cluster 1 of the network were mainly responsible for the lipid metabolic process. Genes in cluster 2 were mainly responsible for olfactory transduction. Genes in cluster 3 (*PTPN3*, one transcript of *SPINT1-AS1*, *SPINT1*, *ST14*, and *ESRPI*) were primarily responsible for epithelial cell development and differentiation. The miRNAs (miR-337-3p and miR-202-5p) were identified to play important roles in the tumor endothelial-mesenchymal transition process.

### Effect of the chromosomal position on the expression of DE mRNAs and DE lncRNAs

Gene mutation and gene expression dysregulation contribute to tumor development [29]. In this study, 101 DE mRNAs and 70 DE lncRNAs enriched on chromosomes revealed that seven and five invasive-related genes were located on chromosomes 11 and 12, respectively (Fig. 7). Five up-regulated olfactory receptors (ORs) family genes (*OR51B6*, *OR52E4*, *OR52E8*, *OR52E6*, and *OR52N2*) and two down-regulated genes (*PKP3* and *NRIP3*) were located in the chromosome 11p15 region ( $p$  value  $< 0.001$ ). Down-regulated genes, including *CDC42BPG*, *RHOD*, *EXPH5*, and *ST14*, were located in other regions on chromosome 11. Five dysregulated genes were found in the 12p13 region ( $p$  value  $< 0.01$ ), including three mRNAs (*CCND2*, *KLRD1*, and *CDKN1B*) and two lncRNAs (*CCND2-AS1* and *MIR200CHG*). Among them, *KLRD1* was confirmed to be up-regulated, while the others were down-regulated.

### Identification of potential molecular signatures expression by RT-qPCR

To validate the Illumina sequencing results, the 11 potential molecular signatures were identified by RT-qPCR. The standard curve of those primers showed that the  $R^2$  ranged between 0.980 and 0.998, and efficiency  $E$  of primers ranged between 92.3 and 109.9% (Figure S3). The standard curve exhibited the good amplifying efficiency of each primer. The relative expression level of nine DE genes (*SGK1*, *OR52E4*, *OR52E8*, *OR52E6*, *OR52N2*, *MAGEA6*, *ST8SIA6-AS1*,



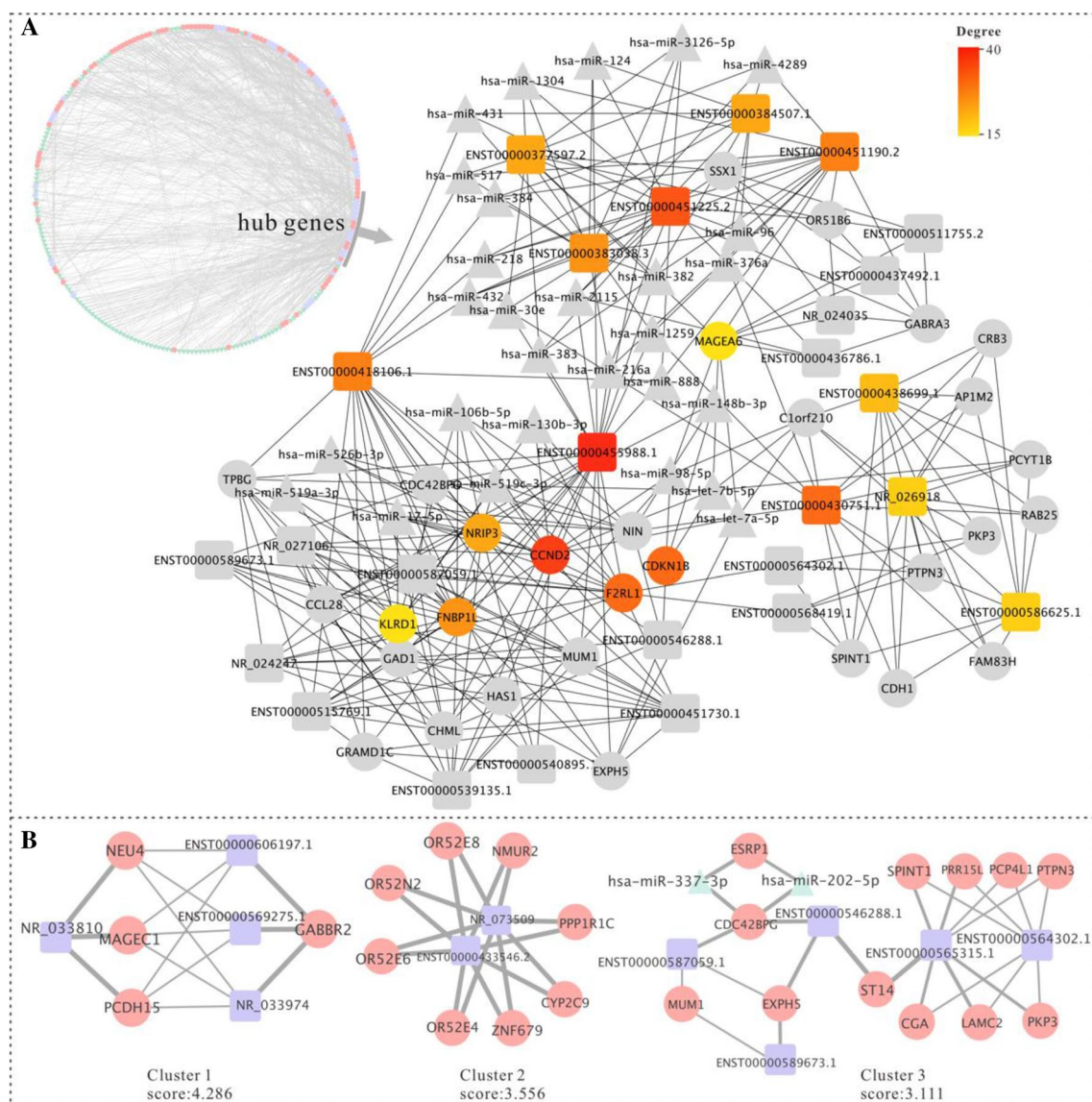


**Fig. 6** CeRNA network and modular analysis. **a** LncRNA-miRNA-mRNA ceRNA network. The nodes in the circle were sorted by their degree. **b** Module analysis of the ceRNA network. The circle represents

the mRNA, the round rectangle represents the lncRNA, and the triangle represents the miRNA

**Table 4** Hub genes in the ceRNA network

Node	Degree	Node	Degree
ENST00000455988.1	38	<i>FNBP1L</i>	20
<i>CCND2</i>	30	ENST00000384507.1	19
ENST00000451225.2	25	ENST00000377597.2	19
ENST00000430751.1	24	<i>NRIP3</i>	19
<i>F2RL1</i>	24	ENST00000438699.1	18
<i>CDKN1B</i>	24	NR_026918	17
ENST00000418106.1	23	ENST00000586625.1	17
ENST00000451190.2	23	<i>KLRD1</i>	16
ENST00000383038.3	20	<i>MAGEA6</i>	16

*SPINT1-AS1*, and *GAD1-AS1*) reflected the same results as predicted by the bioinformatics analysis presented above, illustrating the significantly differentially expressed genes between invasive and non-invasive GH-PAs (Figure S2). *OR51B6* and *MAGEC1* were not significantly differentially expressed ( $p$  value > 0.05).

## Discussion

Invasiveness is a key factor restricting therapeutic effects in patients with GH-PAs. Therefore, it is important to explore the molecular mechanism of GH-PAs' invasion. In this

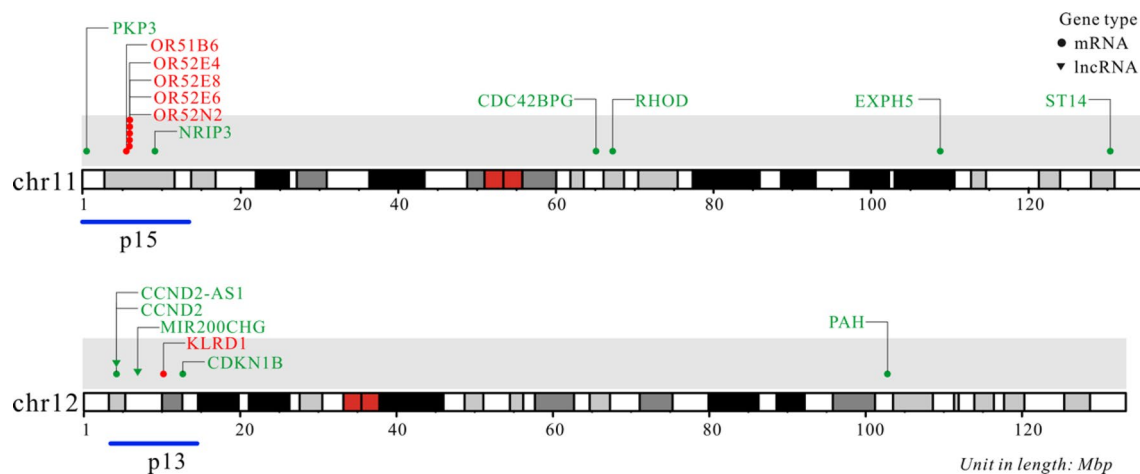


**Fig. 7** Chromosomal position of DE mRNAs and lncRNAs associated with GH-PAs. Red indicates up-regulated genes and green indicates down-regulated genes

study, the DE genes of six GH-PA patients were analyzed based on the invasive and non-invasive characteristics of their tumors. A total of 101 DE mRNAs and 70 DE lncRNAs were identified in invasive GH-PAs. Bioinformatics methods such as GO and KEGG pathway enrichment, PPI and ceRNA network construction, and chromosomal position effect on gene expression were used to explore the biological functions of these DE mRNAs and lncRNAs. Eight DE mRNAs and three DE lncRNAs were found to influence the invasiveness of GH-PAs through aberrant expression of intermediate genes.

Similar to previous findings, some DE mRNAs identified by our transcriptomics research showed aberrant expression in the GH-PAs. Lekva et al. found that decreased expression of epithelial splicing regulator protein 1 (*ESRP1*) might be positively related to the invasiveness of GH-PAs and further increase the epithelial-mesenchymal transition of tumor cells in vitro [30, 31]. Moreover, other genes have been considered to be involved in the development of pituitary tumors, such as *CCND2*, *CDKN1B*, and *GABBR2* [32]. In addition to these reported genes, some new DE mRNAs between invasive and non-invasive GH-PAs (e.g. *OR52E8*, *OR52E6*, *OR52E4*, and *SGK1*) were identified in this study. However, the functions of these genes in GH-PAs require further analysis.

Based on pathway enrichment analysis, top genes of ORs family were significantly up-regulated (*OR52E8*, *OR52E6*, *OR52N2*, and *OR52E4*). Furthermore, the olfactory transduction pathway showed an activity trend in invasive GH-PAs. Other ORs family genes (*OR51E2* and *OR51E1*) were overexpressed in invasive prostate cancer [33, 34] and breast cancer [35, 36]; however, they were never reported in GH-PAs. In our study, four ORs genes showed complex interactions and clustered in a module in the ceRNA network. This

further supports that these genes play an important role in GH-PAs invasion.

Significantly up-regulated MAGE genes (*MAGEC1*, *MAGEC2*, *MAGEA6*, and *MAGEA3*) have been reported to play a prominent role in driving tumorigenesis (especially *MAGEA6* and *MAGEA3*), which is associated with aggressive cancers [37]. It has been reported that less frequent and lower-degree methylation of the *MAGEA3* DNA promoter led to a higher concentration of *MAGEA3* in pituitary tumors than in normal pituitary tissues [38]. This suggests the oncogenic role of *MAGEA3* in pituitary tumors; however, it is unclear whether the roles of *MAGEC1*, *MAGEC2*, and *MAGEA6* in GH-PAs are similar to that of *MAGEA3* in invasive tumors. In ceRNA network analysis, *MAGEA6* was more connected to other genes than *MAGEA3* in GH-PAs, and according to the network module cluster, *MAGEC1* was found to be involved in the lipid metabolic process. This indicates that *MAGEA6* and *MAGEC1* are playing a role in the invasiveness of GH-PAs.

In the PPI network, the hub gene *RHOD* showed significantly decreased expression levels in invasive non-functioning PAs [39]. *CDH1* was down-regulated in aggressive PAs, and its loss on the cell surface is related to the invasiveness of several malignant tumors of epithelial origin [40]. The expression of *CDKN1B* is inversely correlated with the Ki-67-labeling index and under-expression of *CDKN1B* can result in a pituitary hyperplasia and tumorigenesis [41]. In addition to the aforementioned hub genes, *SGK1* was involved in the PI3K oncogenic pathway, which mediates tumor development [42]. However, the potential role of *SGK1* in GH-PAs remains unclear. Liu et al. revealed that inhibition of *SGK1* in prostate cancer epithelial cells suppressed cell invasion, migration, and endothelial-mesenchymal transition processes [43]. Therefore,

up-regulation of *SGK1* may contribute to the development of tumor-invasion ability of GH-PAs.

Multiple studies have shown that lncRNAs play important regulatory roles in tumors [44–46]. Up-regulation of *ST8SIA6-AS1* presented the highest transcript number and expression in invasive tumors. Fang et al. found that *ST8SIA6-AS1* increased the proliferation, migration, and invasion of breast cancer through the p38 MAPK signaling pathway [47]. In this study, the transcripts of *ST8SIA6-AS1* hub gene showed a high correlation with the transcripts of other genes, such as *OR51B6* and *MAGE6*. Considering that these two genes can contribute to worsening the tumor, *ST8SIA6-AS1* may regulate the expression of these two genes and jointly contribute to the development of GH-PAs. For down-regulated lncRNAs, the transcript levels of *GAD1-AS1* and *SPINT1-AS1* were high. The complex ceRNA network showed that *GAD1-AS1* had the most correlations with other genes. As a novel transcript, it is not clear what are its roles and what molecular mechanisms interact in the tumor. *GAD1-AS1* may play a key role in tumor-inhibition and transcripts ENST00000455988.1 and ENST00000418106.1, could serve as a potential index for the diagnosis or prognosis of an invasive GH-PAs. As some reports showed that decreased expression of *SPINT1-AS1* may be independent of unfavorable prognostic indicators in esophageal squamous cell carcinoma [48], we suggest that decreased expression of *SPINT1-AS1* can serve as an indicator of invasive GH-PAs candidate independent of the unfavorable prognostic.

Chromosomal alterations in special loci can lead to dysregulation of prominent oncogenes that drive tumorigenesis [49]. Previous reports suggested that aberrant expression of genes located on the chromosome locus (e.g. 1p11.2) is associated with tumor invasion [29]. According to genome-wide linkage reports, the chr11p15.5 and chr12p13 regions play vital roles in the tumorigenesis of PAs. Under-expression of *CDKN1B*, located in the chr12p13 region, [39–41] and up-regulation of *CD151* and lncRNA *H19*, located on chr11p15.5, have been previously associated with tumorigenesis and involved in the invasion of PAs [50, 51]. Some studies showed that the chr11p15.4 locus is related to tumor invasiveness [52, 53]. However, in invasive GH-PAs, the aberrantly expressed genes located in chr11p15.4 region have not been previously reported. Therefore, based on the enrichment of five ORs genes in the chr11p15.4 region, we hypothesized that genes located in this region also contribute to the invasiveness of GH-PAs. The chromosome 11p15 region of invasive GH-PAs should be further examined.

## Conclusions

To investigate the gene expression profiles of invasive tumors from GH-PAs patients, RNA-seq analysis and systematic bioinformatics approaches were used. A total of 101 mRNAs and 70 lncRNAs showing significant differential expression have been identified between invasive and non-invasive GH-PAs. Further analysis revealed that 11 DE genes were instrumental in the invasiveness of GH-PAs. The up-regulation of *SGK1*, ORs (*OR51B6*, *OR52E4*, *OR52E8*, *OR52E6*, and *OR52N2*), *MAGEA6*, *MAGEC1*, *ST8SIA6-AS1*, and down-regulation of *SPINT1-AS1* and *GAD1-AS1* genes were significantly different in invasive compared to non-invasive GH-PAs. These potential molecular signatures may play crucial roles in the pathogenesis of invasive GH-PAs. However, the small sample size represents the main limitation of this study thus, future studies of larger sample sizes are needed to confirm our results.

**Acknowledgments** We want to thank and acknowledge all participants of the study.

**Funding** This work was funded by the National Natural Science Foundation of China (81801369), Natural Science Foundation of Chongqing (No.cstc2019jcyj-msxmX0475), Nursery Project of Army Medical University (No.2019R054), and Clinical Research Project of Army Military Medical University (2018XLC3049).

**Data availability** The data files can be downloaded from <https://github.com/HuaChunY/GH-PA>. The datasets are available from the corresponding author upon reasonable request.

## Compliance with ethical standards

**Conflicts of interest** The authors declare that there is no conflict of interest.

**Ethics approval** The collection procedure of patient tissue samples in this study was approved by laboratory animal welfare and ethics committee of Xinqiao Hospital (the ethical review number: 2018-049-012). All procedures performed involving human participants were in accordance with the ethical standards of the institutional and/or national research committee and the 1964 Helsinki Declaration and its later amendments or comparable ethical standards.

**Consent to participate** Informed consent was obtained from all participants included in the study.

## References

1. Melmed S (2020) Pituitary-tumor endocrinopathies. *N Engl J Med* 382(10):937–950. <https://doi.org/10.1056/NEJMr1810772>
2. Cuevas-Ramos D, Carmichael JD, Cooper O, Bonert VS, Gertych A, Mamelak AN, Melmed S (2015) A structural and functional acromegaly classification. *J Clin Endocrinol Metab* 100(1):122–131. <https://doi.org/10.1210/jc.2014-2468>



3. Thapar K, Kovacs K, Scheithauer BW, Stefaneanu L, Horvath E, Pernicone PJ, Murray D, Laws ER Jr (1996) Proliferative activity and invasiveness among pituitary adenomas and carcinomas: an analysis using the MIB-1 antibody. *Neurosurgery* 38(1):99–106. <https://doi.org/10.1097/00006123-199601000-00024> (**discussion 106-107**)
4. Zheng X, Li S, Zhang W, Zang Z, Hu J, Yang H (2016) Current biomarkers of invasive sporadic pituitary adenomas. *Ann Endocrinol (Paris)* 77(6):658–667. <https://doi.org/10.1016/j.ando.2016.02.004>
5. Zheng X, Li S, Zang Z, Hu J, An J, Pei X, Zhu F, Zhang W, Yang H (2016) Evidence for possible role of toll-like receptor 3 mediating virus-induced progression of pituitary adenomas. *Mol Cell Endocrinol* 426:22–32. <https://doi.org/10.1016/j.mce.2016.02.009>
6. An J, Zhang Y, He J, Zang Z, Zhou Z, Pei X, Zheng X, Zhang W, Yang H, Li S (2017) Lactate dehydrogenase A promotes the invasion and proliferation of pituitary adenoma. *Sci Rep* 7(1):4734. <https://doi.org/10.1038/s41598-017-04366-5>
7. Wang Z, Gerstein M, Snyder M (2009) RNA-Seq: a revolutionary tool for transcriptomics. *Nat Rev Genet* 10(1):57–63. <https://doi.org/10.1038/nrg2484>
8. Barrett T, Troup DB, Wilhite SE, Ledoux P, Rudnev D, Evangelista C, Kim IF, Soboleva A, Tomashevsky M, Edgar R (2007) NCBI GEO: mining tens of millions of expression profiles database and tools update. *Nucleic Acids Res* 35(Database issue):D760–D765. <https://doi.org/10.1093/nar/gkl887>
9. Consortium GT, Laboratory DA, Coordinating Center -Analysis Working G, Statistical Methods groups-Analysis Working G, Enhancing Gg, Fund NIHC, Nih/Nci, Nih/Nhgri, Nih/Nimh, Nih/Nida, Biospecimen Collection Source Site N, Biospecimen Collection Source Site R, Biospecimen Core Resource V, Brain Bank Repository-University of Miami Brain Endowment B, Leidos Biomedical-Project M, Study E, Genome Browser Data I, Visualization EBI, Genome Browser Data I, Visualization-Ucsc Genomics Institute UoCSC, Lead a, Laboratory DA, Coordinating C, management NIHp, Biospecimen c, Pathology, e QTLmwg, Battle A, Brown CD, Engelhardt BE, Montgomery SB (2017) Genetic effects on gene expression across human tissues. *Nature* 550(7675):204–213. <https://doi.org/10.1038/nature24277>
10. Hochberg I, Harvey I, Tran QT, Stephenson EJ, Barkan AL, Saltiel AR, Chandler WF, Bridges D (2015) Gene expression changes in subcutaneous adipose tissue due to Cushing's disease. *J Mol Endocrinol* 55(2):81–94. <https://doi.org/10.1530/JME-15-0119>
11. Neou M, Villa C, Armignacco R, Jouinot A, Raffin-Sanson ML, Septier A, Letourneur F, Diry S, Diedisheim M, Izac B, Gaspar C, Perlemoine K, Verjus V, Bernier M, Boulin A, Emile JF, Bertagna X, Jaffrezic F, Laloe D, Baussart B, Bertherat J, Gailard S, Assie G (2020) Pangenomic classification of pituitary neuroendocrine tumors. *Cancer Cell* 37(1):123–134.e125. <https://doi.org/10.1016/j.ccell.2019.11.002>
12. Cox MP, Peterson DA, Biggs PJ (2010) SolexaQA: At-a-glance quality assessment of Illumina second-generation sequencing data. *BMC Bioinformatics* 11:485. <https://doi.org/10.1186/1471-2105-11-485>
13. Trapnell C, Pachter L, Salzberg SL (2009) TopHat: discovering splice junctions with RNA-Seq. *Bioinformatics* 25(9):1105–1111. <https://doi.org/10.1093/bioinformatics/btp120>
14. Trapnell C, Williams BA, Pertea G, Mortazavi A, Kwan G, van Baren MJ, Salzberg SL, Wold BJ, Pachter L (2010) Transcript assembly and quantification by RNA-Seq reveals unannotated transcripts and isoform switching during cell differentiation. *Nat Biotechnol* 28(5):511–515. <https://doi.org/10.1038/nbt.1621>
15. Lee CM, Barber GP, Casper J, Clawson H, Diekhans M, Gonzalez JN, Hinrichs AS, Lee BT, Nassar LR, Powell CC, Raney BJ, Rosenbloom KR, Schmelter D, Speir ML, Zweig AS, Haussler D, Haeussler M, Kuhn RM, Kent WJ (2020) UCSC genome browser enters 20th year. *Nucleic Acids Res* 48(D1):D756–D761. <https://doi.org/10.1093/nar/gkz1012>
16. Lopes MBS (2017) The 2017 World Health Organization classification of tumors of the pituitary gland: a summary. *Acta Neuropathol* 134(4):521–535. <https://doi.org/10.1007/s00401-017-1769-8>
17. Robinson MD, McCarthy DJ, Smyth GK (2010) edgeR: a Bioconductor package for differential expression analysis of digital gene expression data. *Bioinformatics* 26(1):139–140. <https://doi.org/10.1093/bioinformatics/btp616>
18. Chen J, Bardes EE, Aronow BJ, Jegga AG (2009) ToppGene suite for gene list enrichment analysis and candidate gene prioritization. *Nucleic Acids Res* 37(Web Server issue):W305–W311. <https://doi.org/10.1093/nar/gkp427>
19. Walter W, Sanchez-Cabo F, Ricote M (2015) GOplot: an R package for visually combining expression data with functional analysis. *Bioinformatics* 31(17):2912–2914. <https://doi.org/10.1093/bioinformatics/btv300>
20. Nie X, Wei J, Hao Y, Tao J, Li Y, Liu M, Xu B, Li B (2019) Consistent biomarkers and related pathogenesis underlying asthma revealed by systems biology approach. *Int J Mol Sci*. <https://doi.org/10.3390/ijms20164037>
21. Zhou G, Soufan O, Ewald J, Hancock REW, Basu N, Xia J (2019) NetworkAnalyst 3.0: a visual analytics platform for comprehensive gene expression profiling and meta-analysis. *Nucleic Acids Res* 47(W1):W234–W241. <https://doi.org/10.1093/nar/gkz240>
22. Su G, Morris JH, Demchak B, Bader GD (2014) Biological network exploration with Cytoscape 3. *Curr Protoc Bioinformatics* 47:8–13. <https://doi.org/10.1002/0471250953.bi0813s47>
23. Paci P, Colombo T, Farina L (2014) Computational analysis identifies a sponge interaction network between long non-coding RNAs and messenger RNAs in human breast cancer. *BMC Syst Biol* 8:83. <https://doi.org/10.1186/1752-0509-8-83>
24. Chin CH, Chen SH, Wu HH, Ho CW, Ko MT, Lin CY (2014) cytoHubba: identifying hub objects and sub-networks from complex interactome. *BMC Syst Biol* 8(Suppl 4):S11. <https://doi.org/10.1186/1752-0509-8-S4-S11>
25. Bader GD, Hogue CW (2003) An automated method for finding molecular complexes in large protein interaction networks. *BMC Bioinformatics* 4:2. <https://doi.org/10.1186/1471-2105-4-2>
26. Subramanian A, Tamayo P, Mootha VK, Mukherjee S, Ebert BL, Gillette MA, Paulovich A, Pomeroy SL, Golub TR, Lander ES, Mesirov JP (2005) Gene set enrichment analysis: a knowledge-based approach for interpreting genome-wide expression profiles. *Proc Natl Acad Sci U S A* 102(43):15545–15550. <https://doi.org/10.1073/pnas.0506580102>
27. Gel B, Serra E (2017) karyoploteR: an R/Bioconductor package to plot customizable genomes displaying arbitrary data. *Bioinformatics* 33(19):3088–3090. <https://doi.org/10.1093/bioinformatics/btx346>
28. van Rijn SJ, Riemers FM, van den Heuvel D, Wolfswinkel J, Hofland L, Meij BP, Penning LC (2014) Expression stability of reference genes for quantitative RT-PCR of healthy and diseased pituitary tissue samples varies between humans, mice, and dogs. *Mol Neurobiol* 49(2):893–899. <https://doi.org/10.1007/s12035-013-8567-7>
29. Thomas G, Jacobs KB, Kraft P, Yeager M, Wacholder S, Cox DG, Hankinson SE, Hutchinson A, Wang Z, Yu K, Chatterjee N, Garcia-Closas M, Gonzalez-Bosquet J, Prokunina-Olsson L, Orr N, Willett WC, Colditz GA, Ziegler RG, Berg CD, Buys SS, McCarty CA, Feigelson HS, Calle EE, Thun MJ, Diver R, Prentice R, Jackson R, Kooperberg C, Chlebowski R, Lissowska J, Peplonska B, Brinton LA, Sigurdson A, Doody M, Bhatti P, Alexander BH, Buring J, Lee IM, Vatten LJ, Hveem K, Kumle M, Hayes RB, Tucker M, Gerhard DS, Fraumeni JF Jr, Hoover RN, Chanock SJ, Hunter DJ (2009) A multistage genome-wide association study in



- breast cancer identifies two new risk alleles at 1p11.2 and 14q24.1 (RAD51L1). *Nat Genet* 41(5):579–584. <https://doi.org/10.1038/ng.353>
30. Lekva T, Berg JP, Lyle R, Heck A, Ringstad G, Olstad OK, Michelsen AE, Casar-Borota O, Bollerslev J, Ueland T (2013) Epithelial splicing regulator protein 1 and alternative splicing in somatotroph adenomas. *Endocrinology* 154(9):3331–3343. <https://doi.org/10.1210/en.2013-1051>
  31. Lekva T, Berg JP, Fougner SL, Olstad OK, Ueland T, Bollerslev J (2012) Gene expression profiling identifies ESRP1 as a potential regulator of epithelial mesenchymal transition in somatotroph adenomas from a large cohort of patients with acromegaly. *J Clin Endocrinol Metab* 97(8):E1506–1514. <https://doi.org/10.1210/jc.2012-1760>
  32. Bujko M, Kober P, Boresowicz J, Rusetska N, Paziewska A, Dabrowska M, Piascik A, Pekul M, Zielinski G, Kunicki J, Bonicki W, Ostrowski J, Siedlecki JA, Maksymowicz M (2019) USP8 mutations in corticotroph adenomas determine a distinct gene expression profile irrespective of functional tumour status. *Eur J Endocrinol* 181(6):615–627. <https://doi.org/10.1530/EJE-19-0194>
  33. Neuhaus EM, Zhang W, Gelis L, Deng Y, Noldus J, Hatt H (2009) Activation of an olfactory receptor inhibits proliferation of prostate cancer cells. *J Biol Chem* 284(24):16218–16225. <https://doi.org/10.1074/jbc.M109.012096>
  34. Rodriguez M, Luo W, Weng J, Zeng L, Yi Z, Siwko S, Liu M (2014) PSGR promotes prostatic intraepithelial neoplasia and prostate cancer xenograft growth through NF-kappaB. *Oncogenesis* 3:e114. <https://doi.org/10.1038/onsis.2014.29>
  35. Weber L, Massberg D, Becker C, Altmüller J, Ubrig B, Bonatz G, Wolk G, Philippou S, Tannapfel A, Hatt H, Gisselmann G (2018) Olfactory receptors as biomarkers in human breast carcinoma tissues. *Front Oncol* 8:33. <https://doi.org/10.3389/fonc.2018.00033>
  36. Masjedi S, Zwiebel LJ, Giorgio TD (2019) Olfactory receptor gene abundance in invasive breast carcinoma. *Sci Rep* 9(1):13736. <https://doi.org/10.1038/s41598-019-50085-4>
  37. Weon JL, Potts PR (2015) The MAGE protein family and cancer. *Curr Opin Cell Biol* 37:1–8. <https://doi.org/10.1016/j.ceb.2015.08.002>
  38. Yacqub-Usman K, Richardson A, Duong CV, Clayton RN, Farrell WE (2012) The pituitary tumour epigenome: aberrations and prospects for targeted therapy. *Nat Rev Endocrinol* 8(8):486–494. <https://doi.org/10.1038/nrendo.2012.54>
  39. Cheng S, Xie W, Miao Y, Guo J, Wang J, Li C, Zhang Y (2019) Identification of key genes in invasive clinically non-functioning pituitary adenoma by integrating analysis of DNA methylation and mRNA expression profiles. *J Transl Med* 17(1):407. <https://doi.org/10.1186/s12967-019-02148-3>
  40. Qian ZR, Sano T, Yoshimoto K, Asa SL, Yamada S, Mizusawa N, Kudo E (2007) Tumor-specific downregulation and methylation of the CDH13 (H-cadherin) and CDH1 (E-cadherin) genes correlate with aggressiveness of human pituitary adenomas. *Mod Pathol* 20(12):1269–1277. <https://doi.org/10.1038/modpathol.3800965>
  41. Seltzer J, Ashton CE, Scotton TC, Pangal D, Carmichael JD, Zada G (2015) Gene and protein expression in pituitary corticotroph adenomas: a systematic review of the literature. *Neurosurg Focus* 38(2):E17. <https://doi.org/10.3171/2014.10.FOCUS14683>
  42. Orlacchio A, Ranieri M, Brave M, Arciuch VA, Forde T, De Martino D, Anderson KE, Hawkins P, Di Cristofano A (2017) SGK1 is a critical component of an AKT-independent pathway essential for PI3K-mediated tumor development and maintenance. *Cancer Res* 77(24):6914–6926. <https://doi.org/10.1158/0008-5472.CAN-17-2105>
  43. Liu W, Wang X, Wang Y, Dai Y, Xie Y, Ping Y, Yin B, Yu P, Liu Z, Duan X, Liao Z, Chen Y, Liu C, Li X, Tao Z (2018) SGK1 inhibition-induced autophagy impairs prostate cancer metastasis by reversing EMT. *J Exp Clin Cancer Res* 37(1):73. <https://doi.org/10.1186/s13046-018-0743-1>
  44. Chiu HS, Somvanshi S, Patel E, Chen TW, Singh VP, Zorman B, Patil SL, Pan Y, Chatterjee SS, Cancer Genome Atlas Research N, Sood AK, Gunaratne PH, Sumazin P (2018) Pan-cancer analysis of lncRNA regulation supports their targeting of cancer genes in each tumor context. *Cell Rep* 23(1):297–3122.e12. <https://doi.org/10.1016/j.celrep.2018.03.064>
  45. Zhang H, Wang Z, Wu J, Ma R, Feng J (2019) Long noncoding RNAs predict the survival of patients with colorectal cancer as revealed by constructing an endogenous RNA network using bioinformatics analysis. *Cancer Med* 8(3):863–873. <https://doi.org/10.1002/cam4.1813>
  46. Jiang N, Wang X, Xie X, Liao Y, Liu N, Liu J, Miao N, Shen J, Peng T (2017) lncRNA DANCER promotes tumor progression and cancer stemness features in osteosarcoma by upregulating AXL via miR-33a-5p inhibition. *Cancer Lett* 405:46–55. <https://doi.org/10.1016/j.canlet.2017.06.009>
  47. Jeong G, Bae H, Jeong D, Ham J, Park S, Kim HW, Kang HS, Kim SJ (2018) A Kelch domain-containing KLHDC7B and a long non-coding RNA ST8SIA6-AS1 act oppositely on breast cancer cell proliferation via the interferon signaling pathway. *Sci Rep* 8(1):12922. <https://doi.org/10.1038/s41598-018-31306-8>
  48. Shen FF, Pan Y, Yang HJ, Li JK, Zhao F, Su JF, Li YY, Tian LQ, Yu PT, Cao YT, Zhang YW, Zhou FY (2019) Decreased expression of SPINT1-AS1 and SPINT1 mRNA might be independent unfavorable prognostic indicators in esophageal squamous cell carcinoma. *Oncotargets Ther* 12:4755–4763. <https://doi.org/10.2147/OTT.S206448>
  49. Dekker J, Mirny L (2016) The 3D genome as moderator of chromosomal communication. *Cell* 164(6):1110–1121. <https://doi.org/10.1016/j.cell.2016.02.007>
  50. Li S, Wu C, Gao H, Wu X, Yu L, Tao B, Hong Y (2018) CD151 up-regulation contributes to the invasion of pituitary adenomas. *Int J Clin Exp Pathol* 11(3):1538–1545
  51. Lu T, Yu C, Ni H, Liang W, Yan H, Jin W (2018) Expression of the long non-coding RNA H19 and MALAT-1 in growth hormone-secreting pituitary adenomas and its relationship to tumor behavior. *Int J Dev Neurosci* 67:46–50. <https://doi.org/10.1016/j.ijdevneu.2018.03.009>
  52. Lv J, Qiu M, Xia W, Liu C, Xu Y, Wang J, Leng X, Huang S, Zhu R, Zhao M, Ji F, Xu L, Xu K, Yin R (2016) High expression of long non-coding RNA SBF2-AS1 promotes proliferation in non-small cell lung cancer. *J Exp Clin Cancer Res* 35:75. <https://doi.org/10.1186/s13046-016-0352-9>
  53. Wang J, Wang H, Liu A, Fang C, Hao J, Wang Z (2015) Lactate dehydrogenase A negatively regulated by miRNAs promotes aerobic glycolysis and is increased in colorectal cancer. *Oncotarget* 6(23):19456–19468. <https://doi.org/10.18632/oncotarget.3318>